APPLIED SCIENCES AND ENGINEERING

Biofuel by isomerizing metathesis of rapeseed oil esters with (bio)ethylene for use in contemporary diesel engines

Kai F. Pfister,[1]* Sabrina Baader,[1]* Mathias Baader,[1] Silvia Berndt,[2] Lukas J. Goossen[3]†

Rapeseed oil methyl ester (RME) and (bio)ethylene are converted into biofuel with an evenly rising boiling point curve, which fulfills the strict boiling specifications prescribed by the fuel standard EN 590 for modern (petro)diesel engines. Catalyzed by a Pd/Ru system, RME undergoes isomerizing metathesis in a stream of ethylene gas, leading to a defined olefin, monoester, and diester blend. This innovative refining concept requires negligible energy input (60°C) and no solvents and does not produce waste. It demonstrates that the pressing challenge of increasing the fraction of renewables in engine fuel may be addressed purely chemically rather than by motor engineering.

INTRODUCTION

The increasing environmental awareness and upcoming shortage of fossil oil have triggered a growing interest in sustainable mobility concepts. A liquid biofuel with high energy density that requires no modification to the millions of existing car, truck, ship, and aircraft engines and that can be distributed within current infrastructure would ideally complement electrical solutions for the mobility of the future (*1*).

Around 80% [107×10^6 metric tons per annum (Mt/a)] of the worldwide plant oil production is required to cover food demands; the remaining 20% are converted into biofuels (11×10^6 Mt/a) or put to industrial use (15×10^6 Mt/a) (*2*, *3*). Biodiesel is presently generated by methanolysis of vegetable oils or animal fats, which transforms the triacylglycerols to fatty acid methyl esters (FAMEs) and glycerol (*4*). In the European Union, a FAME content of 7% in diesel fuel is imposed by European Norm (EN) 590 (*5*), and 10% will be enforced by 2020 (*6*). Besides being a renewable and biodegradable material, biodiesel has beneficial properties over conventional diesel, such as its inherent lubricity, lower sulfur content, and higher flash point. Certain disadvantages, including its instability toward oxidation (*7*), high viscosity and pour point, and increased nitrogen oxide release (*8*), can be tackled with the help of additives (*9*).

The main obstacle to increasing the biodiesel content in motor fuels arises from its unfavorable boiling behavior (*10*). The standard EN 590 for commercial diesel fuel suitable for powering standard diesel engines calls for a smoothly rising boiling point curve within strict limits (Fig. 1) that ensure optimal fuel ignition and combustion. Petrodiesel, which fulfills these requirements, consists of a mixture of linear and branched hydrocarbons with various chain lengths. In contrast, a typical biodiesel based on rapeseed oil methyl ester (RME) mainly contains linear molecules with 19 carbon atoms, that is, 65% methyl oleate [18:1], 22% methyl linoleate [18:2], 8% methyl linolenate [18:3], 1% methyl stearate [18:0], and 4% methyl palmitate [16:0] (*11*). As a result, its boiling range starts at too high a temperature and is disadvantageously narrow (330° to 400°C), clearly outside the EN 590 specifications (Fig. 1). This adversely affects its ignition behavior and precludes late-stage injections as are required by modern diesel engines with particulate filters (*12*–*14*). In pure form, RME and related biodiesels can, thus, only be used in dedicated engines especially engineered to cope with these challenging physical and chemical properties (*15*).

The only known strategy to convert vegetable oils into biofuel suitable for use in standard diesel engines is their conversion into mixtures of saturated hydrocarbons by energy-intensive hydroprocessing (*16*, *17*). Products obtained by conventional cross-metathesis of RME do not meet the specifications of EN 590 (*17*). An alternative, low-temperature refining concept that allows converting vegetable oils into biodegradable product blends with petrodiesel-like boiling ranges would be of tremendous interest. This key challenge is addressed by the isomerizing metatheses process disclosed herein, which enables generating an EN 590–compatible fuel (Fig. 1) from fatty acid esters and ethylene, which is abundantly available from bioethanol or shale gas (*18*).

In isomerizing metatheses, an isomerization catalyst constantly moves double bonds up and down along alkyl chains within a molecule, while an olefin metathesis catalyst continually shuffles the alkyl residues attached to the double bonds between two molecules (*19*–*22*). This iterative, cooperative action of two orthogonal catalysts allows converting single olefins into olefin blends with carbon-chain lengths evenly distributed around the chain length of the starting material. As a technology, isomerizing olefin metathesis has recently made a substantial leap forward from the previous pioneering works in the 1990s (*19*, *23*–*27*). However, it has never been envisaged as a tool for diesel refining. The abundance of potential catalyst poisons in technical-grade plant oils (for example, nitrogen compounds), the incompatibility of multiply unsaturated olefins and of ethylene with isomerization catalysts, the requirement of expensive solvents in most metatheses, and the difficulty to reproducibly tune product distributions are only some of the challenges that seemed to preclude the use of isomerizing metathesis in biodiesel refining. Consequently, no solvent-free isomerizing cross-metathesis of FAMEs and short-chain olefins has been reported to date. When using ethylene and pure methyl oleate in our previously developed isomerizing metathesis process, we were unable to obtain full conversion or homogeneous product distributions even in the presence of solvent (*19*). The corresponding process with unpurified RME or other natural FAMEs suitable for fuel production was, so far, entirely out of reach.

RESULTS

Years of process design led to an effective catalyst system for a simplified model reaction: the isomerizing cross-metathesis of equimolar amounts

[1]Department of Chemistry, Technical University of Kaiserslautern, D-67663 Kaiserslautern, Germany. [2]Fakultät für Maschinenbau und Schiffstechnik, University of Rostock, D-18059 Rostock, Germany. [3]Fakultät für Chemie und Biochemie, Ruhr-Universität Bochum, D-44801 Bochum, Germany.
*These authors contributed equally to this work.
†Corresponding author. Email: lukas.goossen@rub.de

of 1-hexene and unpurified RME from grocery-grade rapeseed oil. In the presence of 0.05 mole percent (mol %) $[Pd(\mu\text{-}Br)(^tBu_3P)]_2$ (**IC-1**) and 0.05 mol % of an N-heterocyclic carbene (NHC)–indenylidene ruthenium complex (**Ru-1**), an even distribution of olefins, monoesters, and diesters formed at 50°C without added solvent (Fig. 2).

Alternative olefin metathesis catalysts were also evaluated, including second-generation indenylidene-ruthenium complexes **Ru-2** and **Ru-3** and Hoveyda-type catalysts **Ru-4**, **Ru-5**, and **Ru-6** (fig. S1). The results obtained are visualized in the superimposed olefin fraction histograms in Fig. 3. The non-isomerized metathesis products decene, tetradecene, and octadecene are overrepresented for all catalyst systems except for the **IC-1**/**Ru-1** combination (black bars with superimposed black trend line). This indicates that all other metathesis catalysts adversely affect the isomerization activity of **IC-1**.

Incorporation of 1-hexene brought about an overall shortening of the chain lengths. As a result, the mixture displayed an evenly rising boiling point curve that closely matches that of petrodiesel in terms of initial and mean boiling points. However, the 1-hexene/RME product showed a recovery of only 93% at 360°C, which narrowly misses the EN 590 specification of 95% (Fig. 1). Toward the end of the distillation, it partially decomposed with smoke formation. This is a common problem for biodiesel caused by oxidation of sensitive polyunsaturated fatty

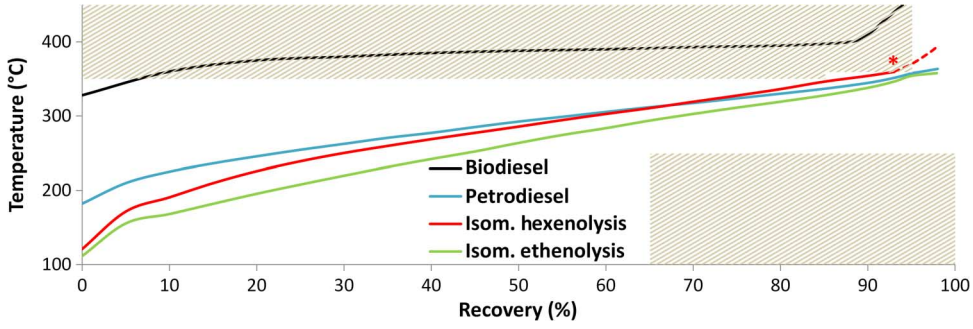

Fig. 1. Boiling point curves of commercial diesel and biodiesel (RME) before and after isomerizing metathesis. The hashed areas represent the limits specified in EN 590. *, increasing decomposition; Recovery, percentage of the sample recovered in the receiving flask during distillation.

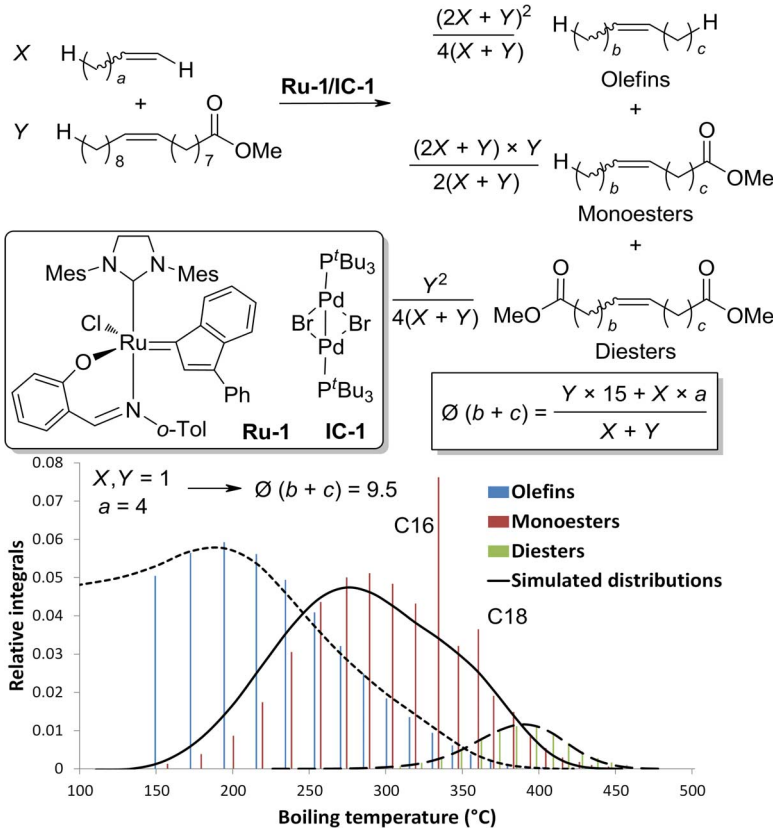

Fig. 2. Boiling point histogram of the product blend after isomerizing hexenolysis of RME. Conditions: 10.0 mmol of 1-hexene/RME (1:1), 0.05 mol % **IC-1** and **Ru-1**, neat, 50°C, 20 hours. The mixture was hydrogenated for analysis. This histogram was overlaid with simulated curves for 1000 molecules per catalyst (≙ 0.05 mol % catalyst) of both 1-hexene and RME, with 30,000 metathesis and 7500 double-bond migration steps. ····, olefins; —, monoesters; – –, diesters.

acid derivatives and is usually addressed by partial hydrogenation of the product fractions (*28*, *29*). This was the best boiling behavior achieved for an isomerizing hexenolysis of RME.

An in-depth understanding of the influence of substrate and process parameters on the boiling behavior was derived from model reactions in combination with arithmetic considerations at equilibrium, and simulations of the reaction course.

At equilibrium, the product distribution for the reaction of X equivalents of 1-hexene and Y equivalents of methyl oleate is governed purely by the relative abundance of C–C double bonds and functionalized and unfunctionalized chain termini. Thus, the ratio of olefins, monoesters, and diesters in the product mixture corresponds to $(2 \times X + Y)^2$:$(2 \times X + Y) \times Y \times 2$:$Y^2$ (Fig. 2). For the reaction of pure methyl oleate ($Y = 1$) with one equivalent of 1-hexene ($X = 1$), the ratio of olefins, monoesters, and diesters following isomerizing hexenolysis should be 9:6:1. The boiling behavior of the product mixture is also influenced by the carbon-chain lengths of the olefin, monoesters, and diester fractions. The mean number of aliphatic carbon atoms per double bond was calculated using the formula Ø $(b + c) = (Y \times 15 + X \times a)/(X + Y)$, with a, b, c, X, and Y as defined in Fig. 2. Two alkene carbons as well as the number of ester termini were added to obtain the mean chain lengths (MCLs). For the isomerizing hexenolysis with one equivalent of 1-hexene, the MCLs of the olefin, monoester, and diester fractions at equilibrium are 11.5, 12.5, and 13.5, respectively. Experimentally, mean values of <12.9 carbons for the olefins [uncorrected for volatiles not detectable by gas chromatography (GC) analysis], 14.4 for the monoesters, and 17.5 for

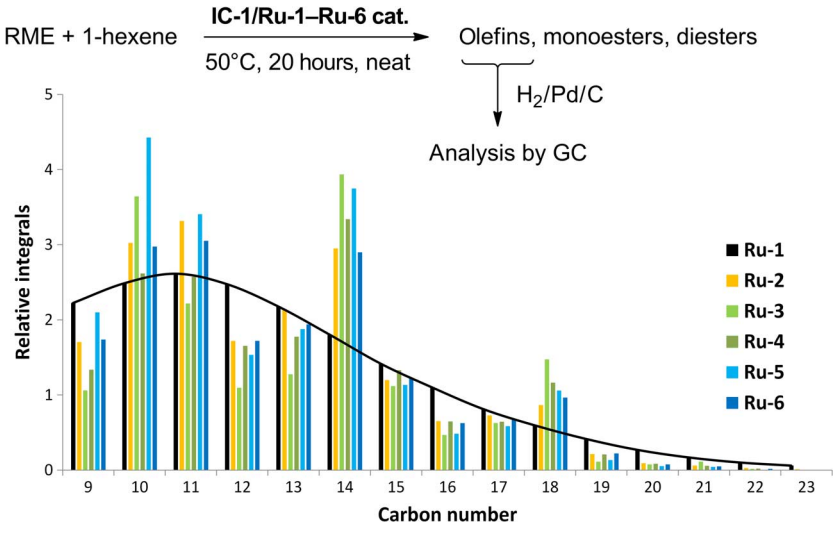

Fig. 3. Carbon-chain length histograms for olefin blends obtained by isomerizing hexenolysis with different Ru catalysts. Conditions: 10.0 mmol of 1-hexene/RME (1:1), 0.05 mol % **IC-1** and **Ru-cat.**, neat, 50°C, 20 hours. The samples were hydrogenated for GC analysis to simplify the chromatograms.

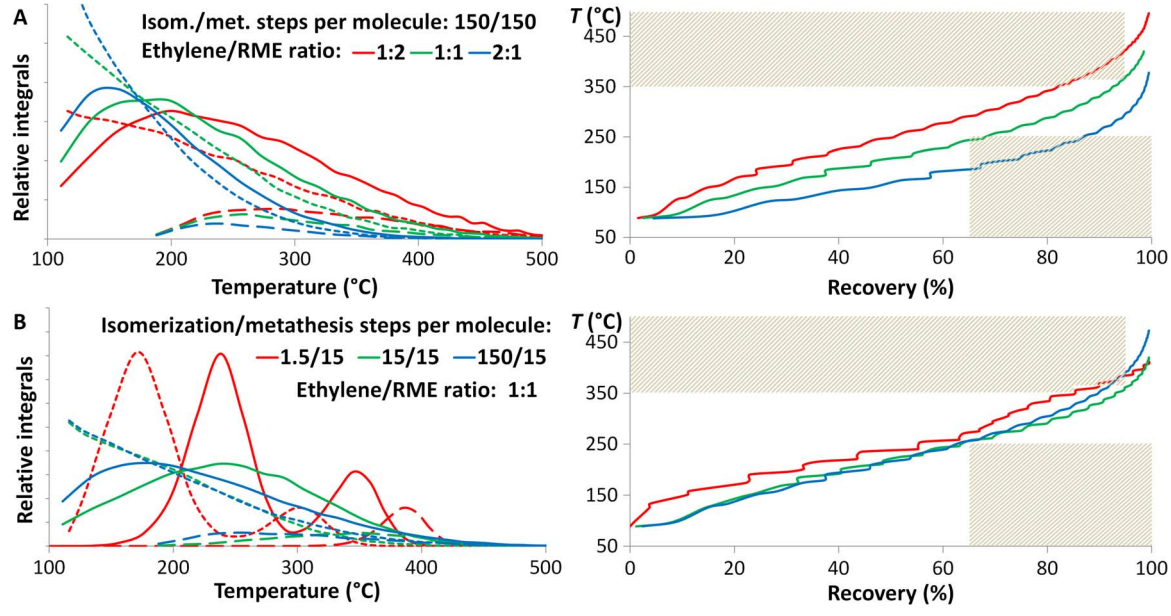

Fig. 4. Simulated boiling point distribution of olefins (····), monoesters (—), and diesters (– –) and boiling point curve of the products after isomerizing ethenolysis. (**A**) Effect of the ethylene/RME ratio near equilibrium and (**B**) effect of the ratio of isomerization/metathesis steps per molecule in preequilibrium reactions. Recovery, percentage of the sample recovered in the receiving flask during distillation analysis.

the diesters were detected for RME. This indicates that the reaction did not reach equilibrium.

To rationalize the product distributions in preequilibrium mixtures, we developed a simulation program in which a given number of randomly chosen molecules from a mixture of 2000 molecules of methyl oleate/hexene at a given ratio (1:1 in the above case) undergo a single shift of their double bond. Then, another given number of randomly chosen molecules undergo metathesis. These two steps are iterated a given number of times so that different overall and relative turnover numbers for both catalyst systems can be modeled (see the "Simulation of the isomerizing hexenolysis reaction mixtures" in the Supplementary Materials).

The experimental product distribution for the isomerizing hexenolysis of RME (Fig. 2, histograms) fits best with the simulated outcome for an average of 15 metathesis and 3.75 isomerization steps per olefin molecule (Fig. 2, simulated curves). This translates to catalyst turnover numbers of 30,000 for **Ru-1** and 7500 for **IC-1**, which are impressive values for solvent-free reactions. Slight deviations of the calculated product distributions from those experimentally observed were to be expected: The multiply unsaturated fatty acids in RME release short-chain fragments and the saturated components, namely, methyl palmitate (1%) and stearate (4%), cannot undergo isomerizing metathesis, which explains the protruding signals of C16 and C18 esters and the increased integral and MCL of the monoester fraction.

With all the necessary tools in hand, we investigated whether and how it is possible to modulate the boiling point curve of RME by isomerizing cross-metathesis with ethylene so that it would meet the EN 590 specifications. Figure 4A illustrates the predicted effect of the ethylene/RME ratio on the simulated boiling point distribution and net boiling point curve near equilibrium, at 150 isomerization and metathesis steps each per molecule. None of the boiling point curves meet the specifications at both middle and high % recovery. The median boiling temperature is too high at a 1:2 ethylene/RME ratio and too low at a 2:1 ratio. The curves for ratios around 1:1 are closest to the desired profile. The boiling behavior can be adjusted further by changing the number of isomerization and metathesis steps per molecule (Fig. 4B). When setting the metathesis steps to 15 per molecule and gradually increasing the number of isomerizations, the product distributions change from irregular patterns with several chain-length maxima per fraction (<10 isomerization steps) to increasingly broad, smooth product distributions around single maxima. At the same time, the amount of high-boiling long-chain compounds initially decreases, goes through a minimum of 10 isomerization steps per molecule, and then increases again. For an ethylene/RME ratio between 0.7:1 and 1.3:1, the boiling point curve is predicted to meet the specifications with a boiling temperature above the lower threshold at 65% recovery and below the upper threshold at 95% recovery if the number of isomerization steps is between 10 and 30

Table 1. Optimization of the isomerizing ethenolysis of RME. Conditions for entries 3 to 12: 2.50 mmol of RME (based on methyl oleate), ethylene, **Ru-cat.**, **Ru-CAAC**, **IC-1**, neat, 16 hours, 60°C.

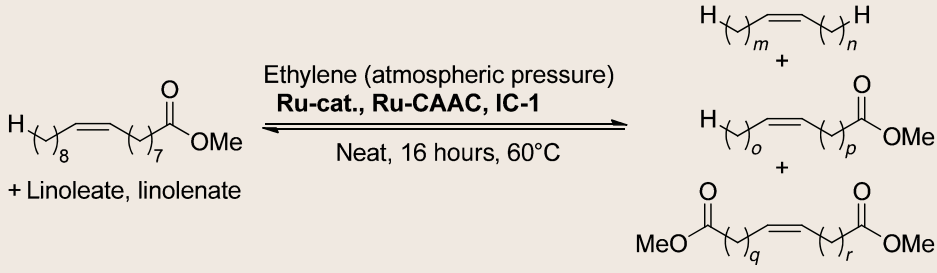

Entry	Ru-cat. (mol %)	Ru-CAAC (mol %)	IC-1 (mol %)	Ethylene (ml)	Reaction temperature (°C)	Average MCL	Evenness of the curve
1	Isomerizing hexenolysis (see above)			—	50	15.0	Excellent
2	Sequential isomerizing ethenolysis			—	50	13.7	Good
3	**Ru-1** (0.05)	—	0.05	300 (at 6 bar)	50	—	No conversion
4	**Ru-1** (0.10)	—	0.10	20	60	18.0	Poor
5	**Ru-5** (0.10)	—	0.10	20	60	15.3	Fair
6	**Ru-7** (0.10)	—	0.10	20	60	15.2	Good
7	**Ru-11** (0.10)	—	0.10	20	60	15.3	Fair
8	**Ru-5** (0.10)	—	0.40	20	60	15.8	Fair
9	**Ru-7** (0.10)	—	0.40	20	60	15.5	Excellent
10	**Ru-11** (0.10)	—	0.40	20	60	15.4	Excellent
11	**Ru-11** (0.10)	0.10	0.40	20	60	15.3	Excellent
12	**Ru-11** (0.10)	0.10	0.40	300 (at 6 bar)	60	14.4	Excellent
13	**Ru-11** (0.10)	0.10	0.40	Constant stream	60	12.9	Excellent

per molecule and if the number of metathesis steps is greater than 7 per molecule. The predicted MCLs for this mixture are 8.6, 11.4, and 14.4 for olefins, monoesters, and diesters, respectively, or 11.5 overall.

Equipped with a link between the physical properties and the chemical composition of the product mixture, as well as an activity profile for the bimetallic catalyst system, we sought suitable catalysts and reaction conditions (see the "Development of the isomerizing ethenolysis of RME" in the Supplementary Materials). The best-known isomerization catalysts, among them the Chaudret, Cole-Hamilton, Behr, Grotjahn/Schrock, and Skrydstrup systems (*20*, *26*, *30*–*33*), were incompatible with ruthenium metathesis catalysts or deactivated by ethylene. **IC-1** was the sole catalyst to display sufficient activity but only at ethylene pressures of ≤1 bar.

IC-1 was evaluated in combination with different metathesis catalysts for the isomerizing ethenolysis of RME (Table 1; see table S4 for full details). The average MCL of the three product fractions was used as a measure of ethylene intake and of the resulting shift toward lower boiling points (cf. figs. S12 to S15 for the effect with 1-hexene). In addition, we evaluated the shape of the product distributions obtained to ensure evenly rising boiling point curves.

Without ethylene, the average MCL is 18 (isomerizing self-metathesis of RME). The isomerizing hexenolysis, used as a further reference point, gave an average MCL of 15 (entry 1). To ensure a defined ratio of RME and ethylene, a two-step process consisting of non-isomerizing ethenolysis of RME followed by isomerizing metathesis of the ethenolyzed product was assessed as a third reference point. This resulted in an average MCL of 13.7 (entry 2). The deviation from the targeted value of 11.5 results from the incorporation of too little ethylene (0.83 rather than one equivalent), a low isomerization rate, difficulties detecting volatile short-chain olefins, and the presence of saturated fatty esters. The experimental boiling point curve measured for this reference material was marginally outside of the EN 590 specifications (see table S5), which confirms that the material has to meet all predicted parameters to reach the targeted behavior.

The system composed of **Ru-1** and **IC-1** was inactive under ethylene pressure, possibly because of decomposition of the ruthenium complex (entry 3). The catalyst loading was increased to 0.10 mol % to compensate for lower activity and stability in the presence of ethylene. Conversion was first observed after switching to atmospheric ethylene pressure (entry 4). Three Ru-NHC complexes (**Ru-5**, **Ru-7**, and **Ru-11**; figs. S1 and S25) mediated the isomerizing metathesis of RME in the presence of ethylene and resulted in almost even product distributions with single maxima (cf. table S4, entries 5 to 7). At an **IC-1** loading further increased to 0.40 mol %, the distributions were more homogeneous, and protruding cross-metathesis products were no longer observed (entries 8 to 10). However, these catalysts incorporated too little ethylene into the product mixture, as visible from the medium chain lengths. We therefore needed to find a highly active ethenolysis catalyst that would retain its activity in the presence of **IC-1.** Fortunately, the complex **Ru-CAAC** described by Marx *et al.* (*34*) was found to be compatible with the isomerizing ethenolysis. However, **Ru-CAAC** did not promote the cross-metathesis of long-chain olefins, leading to the overproportional formation of volatile olefins.

The solution was to combine **IC-1**, **Ru-CAAC**, and **Ru-11** into a mutually compatible, ternary system that is able to catalyze the isomerization, ethenolysis, and long-chain olefin cross-metathesis, respectively. At 60°C, the MCLs reached 14.3, 14.9, and 16.8, respectively (entry 11). Increasing ethylene pressure did not allow the average MCL (entry 12) to sufficiently reduce. However, by running the reaction under a constant stream of ethylene at atmospheric pressure in a specially constructed reactor, the MCLs were further reduced to <12.3, 12.2, and 14.0 carbons for olefins, monoesters, and diesters, respectively (entry 13). These values are close to the MCLs of 8.6, 11.4, and 14.4 predicted by simulation of the optimum product mixture. The gas chromatogram of the experimentally obtained mixture is comparable to that simulated for a 1.3:1 ratio of ethylene/RME, with an average of 15 metathesis and 12 isomerization steps per substrate molecule. This translates to turnover numbers of 15,000 for the metathesis and 3000 for the isomerization catalyst, which is well within the targeted range. Notably, the purity of the ethylene source does not have a significant effect on the catalyst system. When using industrial-grade ethylene (N3.5) in the process, the distributions and MCLs were identical.

The physical properties were experimentally quantified using a product mixture obtained on a larger scale. Thus, 135 ml of RME containing **IC-1** (1.24 g), **Ru-CAAC** (243 mg), and **Ru-11** (330 mg) was stirred under a stream of ethylene at 60°C for 16 hours (Fig. 5). Distillation analysis in an EN ISO (International Organization for Standardization) 3405 apparatus (*35*) furnished an experimental boiling point curve that corresponded well with the prediction derived from the simulation (Figs. 1 and 4). The product blend passed the ASTM (American Society of Testing and Materials) D 6751 boiling specification for biodiesel (*36*), because 90% distilled below 360°C. It also fulfilled all three specifications for petrodiesel fuels laid out in EN 590, namely, a recovery of (i) <65% at 250°C, (ii) >85% at 350°C, and (iii) 95% at ≤360°C. As predicted, the boiling point curve of the ethylene/RME product had a terminal boiling temperature and an overall shape similar to petrodiesel.

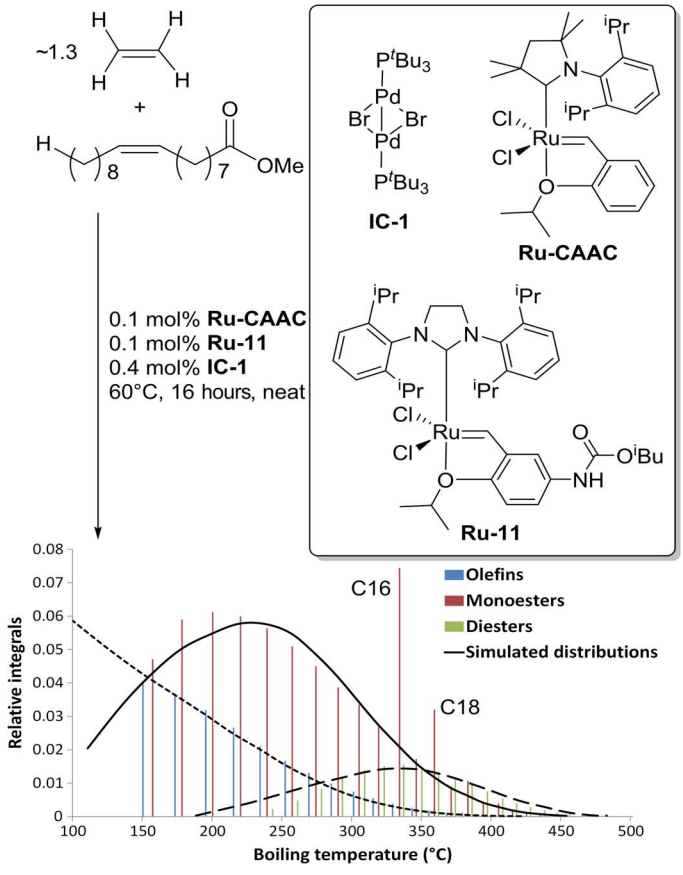

Fig. 5. Isomerizing ethenolysis of RME. Conditions: 400 mmol of RME, ethylene stream, **Ru-11**, **Ru-CAAC**, **IC-1**, neat, 60°C, 16 hours.

In contrast to the 1-hexene/RME product, no decomposition was discernible during distillation of the ethylene/RME product, likely due to the lower content of polyunsaturated fatty acid esters following ethenolysis. Further analysis using standard methods for fuel testing revealed that the material had a sulfur content of <5 mg/kg, a viscosity of 2.12 mm^2/s, and a lubricity of 232 μm, all values well within the EN 590 specifications. The acid value of 0.360 mg of KOH per gram was below the threshold for pure biodiesel. The cloud and pour points, which are not explicitly specified for temperate climatic zones, are significantly below 0°C and, thus, in a good range for unmodified fuel. To demonstrate the new biofuel's suitability as motor fuel, we used it to propel a model diesel car (see movie S1).

DISCUSSION

In conclusion, isomerizing olefin metathesis with (bio)ethylene allows converting RME into olefin mixtures that match the boiling behavior of diesel fuel as specified in EN 590. This technology may turn out to be a decisive breakthrough toward increasing the content of renewables in diesel fuel. The activity, compatibility, and stability of the catalysts are sufficient to demonstrate the viability of this low-temperature refining concept but do not fulfill the industrial manufacturing standards. Many steps are still required to establish an industrial production of an EN 590–compatible biofuel. At the end of this development, we envision a fully continuous flow process in which an RME/ethylene feed passes through alternating sections of immobilized isomerization and metathesis catalysts dimensioned to provide the ideal ratio of turnover frequencies. The limiting challenge at this stage is the discovery of long-lived, economically viable, heterogeneous or heterogenizable catalysts.

MATERIALS AND METHODS

Procedure for the single-stage isomerizing ethenolysis

In a glovebox under nitrogen atmosphere, a 1-liter Parr autoclave was charged with [1-[2,6-bis(1-methylethyl)phenyl]-3,3,5,5-tetramethyl-2-pyrrolidinylidene]dichloro[[2-(1-methylethoxy-κO)phenyl]methylene-κC]-ruthenium(II) (CAS no. 959712-80-2; **Ru-CAAC**, 243 mg, 0.40 mmol), bromo(tri-*tert*-butylphosphine)-palladium(I)dimer (**IC-1**, 1.24 g, 1.60 mmol), Umicore M73 SIPr (**Ru-11**, 330 mg, 0.40 mmol), and RME (135 ml, 400 mmol based on methyl oleate). The autoclave was closed and removed from the glovebox. The resulting reaction mixture was stirred under a stream of ethylene (99.995% purity) at atmospheric pressure for 16 hours at 60°C. The reactor was cooled to ambient temperature, and a 30% solution of H_2O_2 (40.9 ml, 400 mmol) was slowly added at 0°C under vigorous stirring. The organic phase was separated, dried over $MgSO_4$, and filtered over a short column of Celite and $MgSO_4$, yielding 75 ml of a brown oil (55% based on volume). After high-temperature vacuum distillation (1×10^{-3} mbar, >350°C), the product mixture was obtained as a light yellow liquid (73 ml, >98 weight % recovery after distillation).

SUPPLEMENTARY MATERIALS

Supplementary material for this article is available at http://advances.sciencemag.org/cgi/content/full/3/6/e1602624/DC1

Supplementary Materials and Methods

Supplementary Text

fig. S1. Ru-based metathesis catalysts tested in the isomerizing hexenolysis, including second-generation indenylidene-ruthenium complexes Umicore M41 (**Ru-2**) and M31 (**Ru-3**) and Hoveyda-type catalysts Umicore M51 (**Ru-4**), M72 SIMes (**Ru-5**), and M74 SIMes (**Ru-6**).

fig. S2. Olefin blends obtained by isomerizing hexenolysis with different Ru catalysts.

fig. S3. State-of-the-art isomerization catalysts tested in the isomerizing hexenolysis.

fig. S4. Mass-corrected GC with **IC-1**.

fig. S5. Mass-corrected GC with **IC-2**.

fig. S6. Gas chromatogram with **IC-3**.

fig. S7. Gas chromatogram with **IC-4**.

fig. S8. Mass-corrected GC with **IC-5**.

fig. S9. Mass-corrected GC with **IC-6**.

fig. S10. Mass-corrected GC with **IC-7**.

fig. S11. Mass-corrected GC with **IC-8**.

fig. S12. Mass-corrected gas chromatogram with 0 equiv 1-hexene.

fig. S13. Mass-corrected gas chromatogram with 0.3 equiv 1-hexene.

fig. S14. Mass-corrected gas chromatogram with 1 equiv 1-hexene.

fig. S15. Mass-corrected gas chromatogram with 1.5 equiv 1-hexene.

fig. S16. Calculated boiling point curves of RME product blends after isomerizing cross-metathesis with different amounts 1-hexene, along with pure RME and petrodiesel.

fig. S17. Boiling point curves of commercial diesel and biodiesel (RME) before and after isomerizing hexenolysis.

fig. S18. Experimental chain length distributions; MCL: 12.9; 14.4; 17.5.

fig. S19. Simulated distributions; turnover number (TON) M = 30,000; TON I = 7500; MCL: 10.3; 13.8; 17.3.

fig. S20. Simulated distributions; TON M = 30,000; TON I = 15,000; MCL: 10.4; 13.7; 16.8.

fig. S21. Simulated distributions; TON M = 30,000; TON I = 30,000; MCL: 10.5; 13.5; 16.4.

fig. S22. Simulated distributions; TON M = 20,000; TON I = 5,000; MCL: 10.2; 13.8; 17.5.

fig. S23. Simulated distributions; TON M = 40,000; TON I = 10,000; MCL: 10.3; 11.7; 15.1.

fig. S24. Mass-corrected gas chromatogram of the mixture obtained by sequential isomerizing ethenolysis.

fig. S25. Additional Ru-based metathesis catalysts tested in the isomerizing ethenolysis.

fig. S26. Raw gas chromatograms of the product mixture obtained by single-step isomerizing ethenolysis before and after hydrogenation.

fig. S27. Mass-corrected gas chromatogram of the product mixture obtained by single-step isomerizing ethenolysis.

fig. S28. Boiling point curves of commercial diesel and biodiesel (RME) before and after isomerizing ethenolysis.

fig. S29. Experimental chain length distributions; MCL: 12.3; 13.2; 15.7.

fig. S30. Simulated distributions; TON M = 30,000; TON I = 15,000; MCL: 8.9; 12.3; 15.7.

fig. S31. Experimental chain length distributions; MCL: 12.3; 11.8; 13.9.

fig. S32. Simulated distributions; TON M = 15,000; TON I = 3000; MCL: 7.6; 10.6; 13.6.

table S1. Product distributions obtained experimentally by isomerizing hexenolysis of RME.

table S2. Equilibrium product distributions calculated for the isomerizing hexenolysis of RME.

table S3. Comparison of product distributions obtained from isomerizing hexenolysis of RME.

table S4. Optimization of the one-step isomerizing ethenolysis of RME.

table S5. EN ISO 3405 distillation data of isomerizing metathesis reactions with RME.

movie S1. Webra "Winner" 2.5-cm^3 self-igniting model diesel engine operated with the fuel obtained via isomerizing ethenolysis of rapeseed methyl ester.

data file S1. MatLab simulation.

References (*37*–*49*)

REFERENCES AND NOTES

1. Special issue on Sustainability and Energy, *Science* **315** (09 February 2007).
2. P. Gallezot, Conversion of biomass to selected chemical products. *Chem. Soc. Rev.* **41**, 1538–1558 (2012).
3. U. Biermann, U. Bornscheuer, M. A. R. Meier, J. O. Metzger, H. J. Schäfer, Oils and fats as renewable raw materials in chemistry. *Angew. Chem. Int. Ed.* **50**, 3854–3871 (2011).
4. G. Knothe, J. V. Gerpen, *The Biodiesel Handbook, Second Edition* (AOCS Publishing, ed. 2, 2010).
5. European Committee for Standardization (CEN), "Automotive fuels - Diesel - Requirements and test methods" (EN 590, CEN/TC 19, 2014).
6. European Union, Directive 2009/28/EC of the European Parliament and of the Council of 23 April 2009 on the promotion of the use of energy from renewable sources and amending and subsequently repealing directives 2001/77/EC and 2001/30/EC. *OJ L* **140**, 16–62 (2009).
7. G. Knothe, Some aspects of biodiesel oxidative stability. *Fuel Process. Technol.* **88**, 669–677 (2007).
8. M. Lapuerta, O. Armas, J. Rodríguez-Fernández, Effect of biodiesel fuels on diesel engine emissions. *Prog. Energy Combust. Sci.* **34**, 198–223 (2008).
9. N. M. Ribeiro, A. C. Pinto, C. M. Quintella, G. O. da Rocha, L. S. G. Teixeira, L. L. N. Guarieiro, M. do Carmo Rangel, M. C. C. Veloso, M. J. C. Rezende, R. S. da Cruz, A. M. de Oliveira, E. A. Torres, J. B. de Andrade, The role of additives for diesel and diesel blended (ethanol or biodiesel) fuels: A review. *Energy Fuels* **21**, 2433–2445 (2007).
10. C. Bachler, S. Schober, M. Mittelbach, Simulated distillation for biofuel analysis. *Energy Fuels* **24**, 2086–2090 (2010).
11. F. Ma, M. A. Hanna, Biodiesel production: A review. *Bioresour. Technol.* **70**, 1–15 (1999).

12. M. Shahabuddin, A. M. Liaquat, H. H. Masjuki, M. A. Kalam, M. Mofijur, Ignition delay, combustion and emission characteristics of diesel engine fueled with biodiesel. *Renew. Sustain. Energy Rev.* **21**, 623–632 (2013).
13. P. Chen, U. Ibrahim, J. Wang, Experimental investigation of diesel and biodiesel post injections during active diesel particulate filter regenerations. *Fuel* **130**, 286–295 (2014).
14. X. He, A. Williams, E. Christensen, J. Burton, R. McCormick, Biodiesel impact on engine lubricant dilution during active regeneration of aftertreatment systems. *SAE Int. J. Fuels Lubr.* **4**, 158–178 (2011).
15. M. Mofijur, H. H. Masjuki, M. A. Kalam, A. E. Atabani, M. Shahabuddin, S. M. Palash, M. A. Hazrat, Effect of biodiesel from various feedstocks on combustion characteristics, engine durability and materials compatibility: A review. *Renew. Sustain. Energy Rev.* **28**, 441–455 (2013).
16. M. Mittelbach, Fuels from oils and fats: Recent developments and perspectives. *Eur. J. Lipid Sci. Technol.* **117**, 1832–1846 (2015).
17. R. E. Montenegro, M. A. R. Meier, Lowering the boiling point curve of biodiesel by cross-metathesis. *Eur. J. Lipid Sci. Technol.* **114**, 55–62 (2012).
18. R. Höfer, *Sustainable Solutions for Modern Economies*, vol. 4 of *RSC Green Chemistry Series* (RSC Publishing, 2009).
19. D. M. Ohlmann, N. Tschauder, J.-P. Stockis, K. Gooßen, M. Dierker, L. J. Gooßen, Isomerizing olefin metathesis as a strategy to access defined distributions of unsaturated compounds from fatty acids. *J. Am. Chem. Soc.* **134**, 13716–13729 (2012).
20. A. Behr, A. J. Vorholt, K. A. Ostrowski, T. Seidensticker, Towards resource efficient chemistry: Tandem reactions with renewables. *Green Chem.* **16**, 982–1006 (2014).
21. T. L. Lohr, T. J. Marks, Orthogonal tandem catalysis. *Nat. Chem.* **7**, 477–482 (2015).
22. A. S. Goldman, A. H. Roy, Z. Huang, R. Ahuja, W. Schinski, M. Brookhart, Catalytic alkane metathesis by tandem alkane dehydrogenation-olefin metathesis. *Science* **312**, 257–261 (2006).
23. L. Porri, P. Diversi, A. Lucherini, R. Rossi, Catalysts derived from Ruthenium and Iridium for the ring-opening polymerization of cycloolefins. *Makromol. Chem.* **176**, 3121–3125 (1975).
24. M. B. France, J. Feldman, R. H. Grubbs, An Iridium-based catalyst system for metathesis/isomerization of acyclic olefins, including methyl oleate. *J. Chem. Soc. Chem. Commun.* **11**, 1307–1308 (1994).
25. C. S. Consorti, G. L. P. Aydos, J. Dupont, Tandem isomerisation–metathesis catalytic processes of linear olefins in ionic liquid biphasic system. *Chem. Commun.* **46**, 9058–9060 (2010).
26. G. E. Dobereiner, G. Erdogan, C. R. Larsen, D. B. Grotjahn, R. R. Schrock, A one-pot tandem olefin isomerization/metathesis-coupling (ISOMET) reaction. *ACS Catal.* **4**, 3069–3076 (2014).
27. D. Sémeril, C. Bruneau, P. H. Dixneuf, Imidazolium and imidazolinium salts as carbene precursors or solvent for ruthenium-catalysed diene and enyne metathesis. *Adv. Synth. Catal.* **344**, 585–595 (2002).
28. G. Knothe, R. O. Dunn, Dependence of oil stability index of fatty compounds on their structure and concentration and presence of metals. *J. Am. Oil Chem. Soc.* **80**, 1021–1026 (2003).
29. E. N. Frankel, *Lipid Oxidation* (Elsevier, 2014).
30. F. Bouachir, B. Chaudret, F. Dahan, F. Agbossou, I. Tkatchenko, Preparation and stoichiometric and catalytic reactivity of hydrido organometallic ruthenium complexes. X-ray crystal structure of $[RuH(\eta^5\text{-}C_8H_{11})_2]BF_4$. *Organometallics* **10**, 455–462 (1991).
31. C. J. Rodriguez, D. F. Foster, G. R. Eastham, D. J. Cole-Hamilton, Highly selective formation of linear esters from terminal and internal alkenes catalysed by Palladium complexes of bis-(di-*tert*-butylphosphinomethyl)benzene. *Chem. Commun.* **15**, 1720–1721 (2004).
32. D. B. Grotjahn, C. R. Larsen, J. L. Gustafson, R. Nair, A. Sharma, Extensive isomerization of alkenes using a bifunctional catalyst: An alkene zipper. *J. Am. Chem. Soc.* **129**, 9592–9593 (2007).
33. D. Gauthier, A. T. Lindhardt, E. P. K. Olsen, J. Overgaard, T. Skrydstrup, In situ generated bulky Palladium hydride complexes as catalysts for the efficient isomerization of olefins. Selective transformation of terminal alkenes to 2-alkenes. *J. Am. Chem. Soc.* **132**, 7998–8009 (2010).
34. V. M. Marx, A. H. Sullivan, M. Melaimi, S. C. Virgil, B. K. Keitz, D. S. Weinberger, G. Bertrand, R. H. Grubbs, Cyclic alkyl amino carbene (CAAC) Ruthenium complexes as remarkably active catalysts for ethenolysis. *Angew. Chem. Int. Ed.* **54**, 1919–1923 (2015).
35. International Organization for Standardization (ISO), "Petroleum products—Determination of distillation characteristics at atmospheric pressure" (EN ISO 3405, ISO/TC 28, 2011).
36. American Society for Testing and Materials (ASTM), "Standard Specification for Biodiesel Fuel Blend Stock (B100) for Middle Distillate Fuels" (ASTM D 6751c, ASTM, 2015).
37. Envantage Inc., "Dragon SimDist"; www.envantage.com/analytical-software/envantage-analytical-software/dragon-software/dragon-simdist/.
38. A. B. Littlewood, *Gas Chromatography: Principles, Techniques, and Applications* (Academic Press, ed. 2, 1970).
39. P. Mamone, M. F. Grünberg, A. Fromm, B. A. Khan, L. J. Gooßen, $[Pd(\mu\text{-}Br)(P^tBu_3)]_2$ as a highly active isomerization catalyst: Synthesis of enol esters from allylic esters. *Org. Lett.* **14**, 3716–3719 (2012).
40. V. Durà-Vilà, D. M. P. Mingos, R. Vilar, A. J. P. White, D. J. Williams, Reactivity studies of $[Pd_2(\mu\text{-}X)_2(PBu^t_3)_2]$ (X = Br, I) with CNR (R = 2,6-dimethylphenyl), H_2 and alkynes. *J. Organomet. Chem.* **600**, 198–205 (2000).
41. V. Durà-Vilà, D. M. P. Mingos, R. Vilar, A. J. P. White, D. J. Williams, Insertion of O_2 into a Pd(I)–Pd(I) dimer and subsequent C–O bond formation by activation of a C–H bond. *Chem. Commun.* **16**, 1525–1526 (2000).
42. F. Barrios-Landeros, B. P. Carrow, J. F. Hartwig, Autocatalytic oxidative addition of PhBr to $Pd(P^tBu_3)_2$ via $Pd(P^tBu_3)_2(H)(Br)$. *J. Am. Chem. Soc.* **130**, 5842–5843 (2008).
43. A. Behr, D. Obst, A. Westfechtel, Isomerizing hydroformylation of fatty acid esters: Formation of ω-aldehydes. *Eur. J. Lipid Sci. Technol.* **107**, 213–219 (2005).
44. D. M. Ohlmann, L. J. Gooßen, M. Dierker, Regioselective synthesis of β-aryl- and β-amino-substituted aliphatic esters by rhodium-catalyzed tandem double-bond migration/conjugate addition. *Chemistry* **17**, 9508–9519 (2011).
45. Y. Yuki, K. Takahashi, Y. Tanaka, K. Nozaki, Tandem isomerization/hydroformylation/hydrogenation of internal alkenes to *n*-alcohols using Rh/Ru dual- or ternary-catalyst systems. *J. Am. Chem. Soc.* **135**, 17393–17400 (2013).
46. A. J. Rucklidge, G. E. Morris, D. J. Cole-Hamilton, Methoxycarbonylation of vinyl acetate catalysed by palladium complexes of bis(ditertiarybutylphosphinomethyl)benzene and related ligands. *Chem. Commun.* **9**, 1176–1178 (2005).
47. D. Quinzler, S. Mecking, Linear semicrystalline polyesters from fatty acids by complete feedstock molecule utilization. *Angew. Chem. Int. Ed.* **49**, 4306–4308 (2010).
48. S. Manzini, D. J. Nelson, S. P. Nolan, A Highly active cationic ruthenium complex for alkene isomerisation: A catalyst for the synthesis of high value molecules. *ChemCatChem* **5**, 2848–2851 (2013).
49. S. Manzini, J. A. Fernández-Salas, S. P. Nolan, From a decomposition product to an efficient and versatile catalyst: The $[Ru(\eta^5\text{-indenyl})(PPh_3)_2Cl]$ story. *Acc. Chem. Res.* **47**, 3089–3101 (2014).

Acknowledgments: We acknowledge Umicore AG for the donation of chemicals and P. E. Podsiadly, J. Bartel, and A. Bernhardt for the technical assistance. **Funding:** We thank the Deutsche Forschungsgemeinschaft (Collaborative Research Centre SFB/TRR 88 "3MET" and Cluster of Excellence RESOLV, EXC 1069), Carl Zeiss (Zentrum für ressourceneffiziente Chemie und Rohstoffwandel), and the DBU (German Federal Environmental Foundation) (fellowship to S. Baader) for financial support. **Author contributions:** L.J.G. supervised the research, developed the idea of the project, and designed the experiments. K.F.P. and S. Baader designed and carried out experiments and performed the data analysis. M.B. created the simulation algorithm. S. Berndt performed and interpreted the distillation experiments. **Competing interests:** L.J.G., K.F.P., and S. Baader are authors on a patent application related to this work held by Umicore AG and Co. (PAT-160309EPA, application no. 16160396.4-1371, filed 27 September 2016). All other authors declare that they have no competing interests. **Data and materials availability:** All data needed to evaluate the conclusions in the paper are present in the paper and/or the Supplementary Materials. Additional data related to this paper may be requested from the authors.

Submitted 26 October 2016
Accepted 26 April 2017
Published 16 June 2017
10.1126/sciadv.1602624

Citation: K. F. Pfister, S. Baader, M. Baader, S. Berndt, L. J. Goossen, Biofuel by isomerizing metathesis of rapeseed oil esters with (bio)ethylene for use in contemporary diesel engines. *Sci. Adv.* **3**, e1602624 (2017).

Biofuel by isomerizing metathesis of rapeseed oil esters with (bio)ethylene for use in contemporary diesel engines

Kai F. Pfister, Sabrina Baader, Mathias Baader, Silvia Berndt and Lukas J. Goossen

Sci Adv **3** (6), e1602624.
DOI: 10.1126/sciadv.1602624